RESEARCH ACTIVITIES ON A SUPERCRITICAL PRESSURE WATER REACTOR IN KOREA

YOON-YEONG BAE*, JINSUNG JANG, HWAN-YEOL KIM, HAN-YOUNG YOON, HAN-OK KANG and KANG-MOK BAE[1]
Korea Atomic Energy Research Institute
1045 Daedeokdaero Yuseong Daejeon 305-353, Korea
[1]Korea Hydro & Nuclear Power Co, Ltd.
167 Samseong-dong, Gangnam-gu, Seoul 135-791, Korea
*Corresponding author. E-mail : yybae@kaeri.re.kr

Received July 16, 2007

This paper presents the research activities performed to date for the development of a supercritical pressure water-cooled reactor (SCWR) in Korea. The research areas include a conceptual design of an SCWR with an internal flow recirculation, a reactor core conceptual design, a heat transfer test with supercritical CO_2, an adaptation of an existing safety analysis code to the supercritical pressure condition, and an evaluation of candidate materials through a corrosion study. Methods to reduce the cladding temperature are introduced from two different perspectives, namely, thermal-hydraulics and core neutronics. Briefly described are the results of an experiment on the heat transfer at a supercritical pressure, an experiment that is essential for the analysis of the subchannels of fuel assemblies and the analysis of a system safety. An existing system code has been adapted to SCWR conditions, and the process of a first-hand validation is presented. Finally, the corrosion test results of the candidate materials for an SCWR are introduced.

KEYWORDS : Supercritical Pressure, Reactor Core Concept, Convective Heat Transfer, Safety Analysis, Material for High Temperature Service

1. INTRODUCTION

Recently, nuclear industries and research communities have started paying attention to a supercritical pressure water-cooled reactor (SCWR), recognizing its potential to improve economics with a high core outlet temperature while utilizing most of the existing boiling water reactor (BWR) and pressurized water reactor (PWR) technologies as well as those of a fossil power plant operating at a supercritical pressure. The Generation IV International Forum has selected the SCWR design as a viable candidate for Generation IV nuclear systems to be deployed by 2030, especially for economical electricity generation [1].

The current SCWR-related research areas in Korea include the following: a conceptual design of a reactor core, a heat transfer test with supercritical pressure CO_2, the adaptation of an existing safety analysis code to supercritical pressure conditions, and the evaluation and development of a candidate material for the reactor core and internals. The high cladding temperature is said to be a limiting factor for the design of an SCWR. However, flow recirculation in the reactor, as in the BWR, is a possible solution to this problem. A preliminary study on the conceptual design of an SCWR has been performed based on this idea, and the details are presented here. The preliminary study may well have neglected many areas to be considered for the actual design; however, the study will serve as a starting point or will provide one of the ways to resolve the problem of high cladding temperature. A preliminary neutronics calculation for a reactor core with a solid moderator, ZrH_2, showed reasonable results. Several topics, however, such as a relatively high peaking factor and a local hot spot were identified for further research. A refinement of the core design continues in parallel with development of the core thermal-hydraulics. A core with a solid moderator is particularly suited for a simplification of the coolant passages. Basically, the shape of a solid moderator is a cross, and another improved version is being studied. Another area of our research activity is the study of a convective heat transfer at a supercritical pressure with CO_2 as a medium. The experimental study of a heat transfer to CO_2 flowing vertically upward through a tube and an annulus passage has been performed. The results for the tubes and annulus passage are presented here. An adaptation, including an incorporation of fluid properties at a supercritical pressure, and an examination of the robustness of the safety analysis code under SCWR

conditions have been performed. The test for the evolved code, TASS/SCWR, against MARS an established safety analysis code has been proved reasonable. Development of a new material and an evaluation of existing materials for the fuel cladding and structure are another important area to be pursued, since the supercritical pressure and high temperature environment of an SCWR is extremely corrosive and the irradiation characteristics are not very well known for these conditions. At this time, no material has met the requirements for the current SCWR design conditions, and a great deal of effort is being devoted to this area. The prospective candidates include Ni base alloy, high Cr steel, Ferritic/Martensitic steel, and ODS (oxide dispersed steel).

As a MOST-sponsored project, a three-year feasibility study for the development of an SCWR was initiated as of March 1, 2007. At the conclusion of this project, provisions of the rationales, methodology, assessment of infra-structure, and strategies for the development of an SCWR will be presented. The outcome of this project will serve as a basis for establishing a development policy for an SCWR.

The following sections briefly describe the activities associated with current SCWR development in Korea.

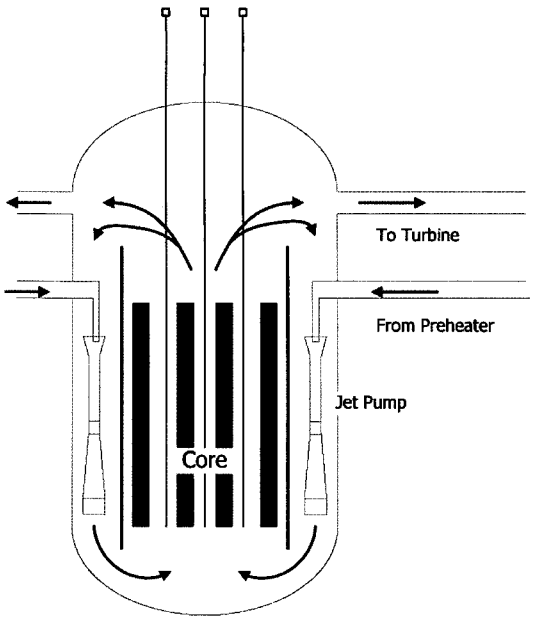

Fig. 1. SCWR-R Design Concept

2. CONCEPTUAL DESIGN OF AN SCWR WITH AN INTERNAL FLOW RECIRCULATION

2.1 Design Concept of the SCWR-R

High-average core outlet temperature is an essential requirement to achieve a high thermal efficiency in an SCWR plant. A cladding oxidation corrosion problem limits an achievable maximum core outlet temperature at the hot channel. The outlet temperature of the hot channel evaluated by Westinghouse for the current once-through SCWR concept was much higher than the allowable maximum cladding temperature [2]. Given this result, Westinghouse concluded that a significant reduction in the core outlet temperature would be required, unless significantly lower hot channel coefficients were considered. Cheng performed a sub-channel analysis on an SCWR using the STAR-SC developed at the Forschungszentrum Karlsruhe [3]. His results also showed that the cladding temperature exceeded the allowable value. He suggested that a modification of the fuel assembly is necessary to keep the cladding surface temperature below the design value.

It is necessary to reduce the enthalpy rise through the core for a high plant thermal efficiency while satisfying the maximum cladding temperature limitation. For this purpose, a new SCWR concept (SCWR-R) with an internal flow recirculation was proposed. In this concept, the overall system will have characteristics similar to a gas-cooled reactor, such as a low density and a high velocity of reactor coolant. Fig. 1 shows the SCWR-R design concept. Jet pumps installed in the downcomer of the reactor cause the coolant to recirculate between the core and the downcomer. The proposed SCWR-R concept is based on the SCLWR-H developed by the University of Tokyo [4]. Geometric parameters, such as the active core height and fuel rod number per assembly are preserved. The core flow rate of the SCWR-R is 6441 kg/s, which is much larger than the reference value of SCLWR-H, at 1816 kg/s. Meanwhile the flow rate and temperature of the feedwater have been evaluated to be 2518 kg/s and 350°C

2.2 Evaluation of the SCWR-R Design Parameters

2.2.1 Simplified Analysis for Fuel Channels

As a preliminary analysis tool for the SCWR-R fuel channel, a simplified one-dimensional thermal-hydraulic code has been developed. Similar to the SCWAT from Westinghouse, this code calculates the hot channel by applying the hot channel factors to the average best estimate channel in a direct way [2]. A cosine axial heat flux profile is assumed for the fuel channels. Bishop's correlation is selected to calculate the cladding temperatures, and the frictional pressure drop is obtained from the correlation proposed by Petrov and Popov [5].

The hot channel factors and uncertainties are from Westinghouse's study, which was based on the CRBRP and Westinghouse's PWR experience [2]. For the hot channel calculation, the flow into each assembly is assumed to match the radial peaking factor exactly so that all the channels behave like an average channel. Only the inlet

flow maldistribution uncertainty among the plant operating parameters is reflected for the hot channel.

Fig. 2 displays the cladding and coolant temperature variations of the hot/average channels for the SCWR-R. In this case, the cladding temperature of the hot channel always remains within the temperature limit, even though the hot channel factors and uncertainties are preserved at the same values. By the introduction of a recirculation concept, a high core exit temperature and a resultant high thermal efficiency are maintained by satisfying the temperature criterion.

For the SCWR-R, the core inlet coolant condition is already beyond the pseudo-critical line, and the coolant properties do not undergo any severe change along the fuel channel. The maximum relative heat flux is about a half of the limit value, which illustrates that the core of the SCWR-R is much safer than that of the reference design from the view point of critical heat flux (CHF). The pressure drop for the average and hot channels are 0.2 MPa and 0.325 MPa, respectively. To obtain the required flow distribution in the core, throttling devices, such as an inlet orifice, should be installed in the fuel channel. The design value of the core pressure drop is 0.325 MPa without consideration of flow oscillation.

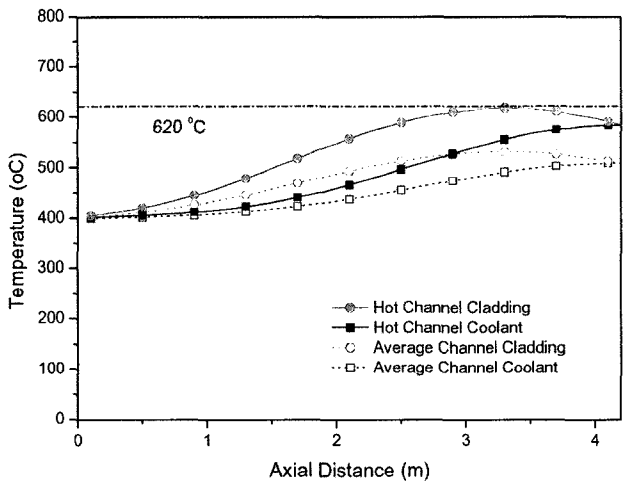

Fig. 2. Cladding and Coolant Temperature Variations of Hot/Average Channels for SCWR-R

2.2.2 Jet Pump Throat Area Sizing

To obtain a high coolant flow rate without an increase of the balance of plant (BOP) components, a "recirculation" concept is suggested in this study. This concept is to install jet pumps at the downcomer and to increase the feedwater pressure to supply a driving momentum for the jet pumps. A recirculation system provides a forced circulating flow through the BWR cores [6]. The system consists of external recirculation pumps, control and isolation valves, and jet pumps installed between the reactor vessel and core shroud. The recirculation pumps pressurize the coolant and send it to the jet pump nozzles.

It is necessary to design a jet pump to achieve the design conditions. The first basic design data, such as the geometric information and the head are taken from the GESSAR II by General Electric [6]. In this study, only the throat area is changed to obtain the design conditions of the SCWR-R, while the other parameters are fixed. The jet pump model of RETRAN is utilized for this calculation [7]. Fig. 3 illustrates the RETRAN control volume representation of a jet pump. The pressure differences between the driving and suction flows at the jet pump with variation of the throat area are calculated. The result is displayed in Fig. 4, which shows that the pressure difference decreases as the throat area increases. As mentioned in the former section, the core pressure difference is 0.325 MPa, from which the necessary pressure difference of the driving flow is determined to be 1.9 MPa with the throat area of 0.00216 m^2. Required

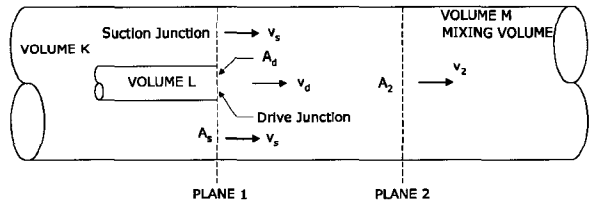

Fig. 3. RETRAN Control Volume Representation of Jet Pump

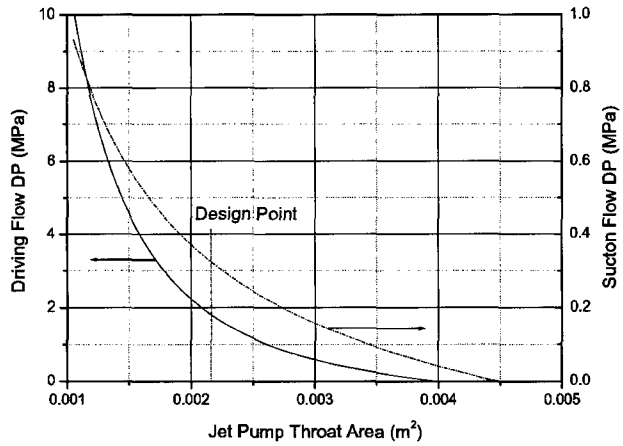

Fig. 4. Pressure Differences of Driving and Suction Flows

additional feedwater pressure is assumed to be 2.0 MPa for the cycle efficiency calculation.

2.2.3 Thermal Efficiency Evaluation

A heat balance calculation is performed for the SCWR-R design conditions. The basic BOP concept here is a two-stage reheating and an eight-stage regenerative system. This setup is based on the system configuration suggested by Dobashi et al. who combined the characteristics of an advanced boiling water reactor (ABWR) designed by General Electric and a supercritical pressure fossil-fired power plant [8].

The steam cycle is equipped with one moisture separator and two reheaters as in the ABWR. High-pressure, intermediate-pressure and low-pressure turbines are used, as in the supercritical pressure fossil-fired power plant. A deaerator is not adopted here because of a concern regarding radioactivity release with the deaeration process. For the heat balance calculation, the important design parameters of the BOP components for thermal efficiencies, such as the turbine isentropic efficiency and pump efficiency, were tuned so that the heat balance results were matched with the ABWR value.

The resultant heat balance of the SCWR-R is shown in Fig. 5. The calculated thermal efficiency is 43.68 %, which is a little lower than the 44 % of the SCLWR-H. While the optimized feedwater inlet temperature was selected for the maximum thermal efficiency in the case of the SCLWR-H, the restriction on the ratio between the core and feedwater flow rates requires the feedwater temperature to be around the pseudo-critical line in this study.

3. CONCEPTUAL DESIGN OF AN SCWR CORE[1)]

3.1 Neutronic Calculation Methods

The HELIOS/MASTER code system was used for the analysis of the SCWR core design concept [9,10]. HELIOS is a two-dimensional neutron transport analysis code using the current coupling collision probability method for a neutron transport calculation. In order to generate few group constants for a core analysis, single fuel assembly calculations for different kinds of fuel assemblies have been performed by the HELIOS code with the 47-neutron group library. MASTER is a three-dimensional nodal core analysis code developed by KAERI, and it is used for the core analysis of the conceptual SCWR

[1)] The conceptual design of an SCWR core described here has been studied independently from the work introduced in Section 2.

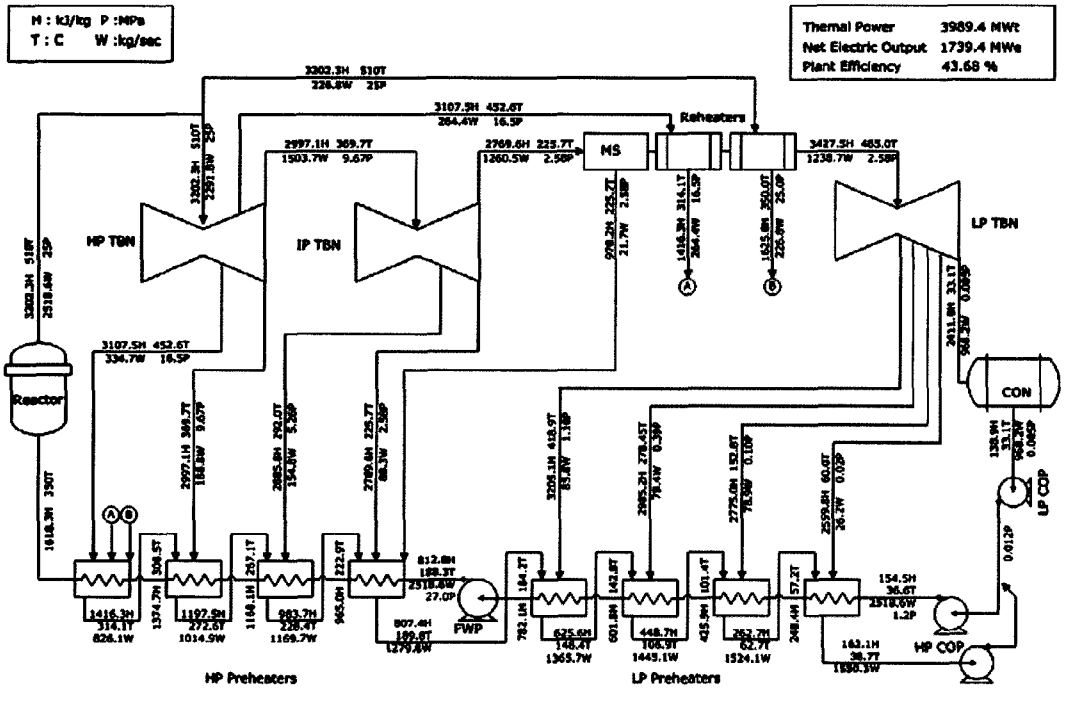

Fig. 5. Result of the Heat Balance Study of the SCWR-R Steam Cycle

core with two-group constants. MASTER considers the thermal-hydraulic feedback effect in the neutronic core calculation by implementing either a simple channel-wise T/H feedback model or a multi-channel T/H analysis like that in COBRA. Since the operating pressure of the SCWR core is above the critical pressure of water, the properties of the water coolant are very different from that of a PWR. Therefore, in order to apply the existing T/H feedback model to the SCWR core analysis, the original steam table used in the MASTER code was substituted by the IAPWS-IF97 steam table.

3.2 Fuel Assembly Design

One of the main characteristic features of an SCWR concept compared with a Light Water Reactor (LWR) is that the average coolant temperature variation along the core height ranges from 280°C to 510°C with a higher pressure of 25 MPa, which is also higher than the critical pressure of 22.1 MPa. Therefore, the water density varies dramatically from ~0.7 g/cm^3 to ~0.1 g/cm^3 under normal operating conditions, and this necessitates an additional moderator in order to slow down the fission neutrons for the SCWR core to have a thermal neutron spectrum. Fig. 6 shows the conceptual design of the SCWR fuel assembly. A cruciform-type solid moderator was proposed for the rectangular fuel assembly design to have a thermal neutron spectrum [11]. The material of the solid moderator is ZrH_2, which was the best moderation material, as determined from the INL research work on solid moderator candidates [12]. The fuel assembly has a 21×21 fuel rods array with a pitch of 1.15 cm, and the fuel assembly

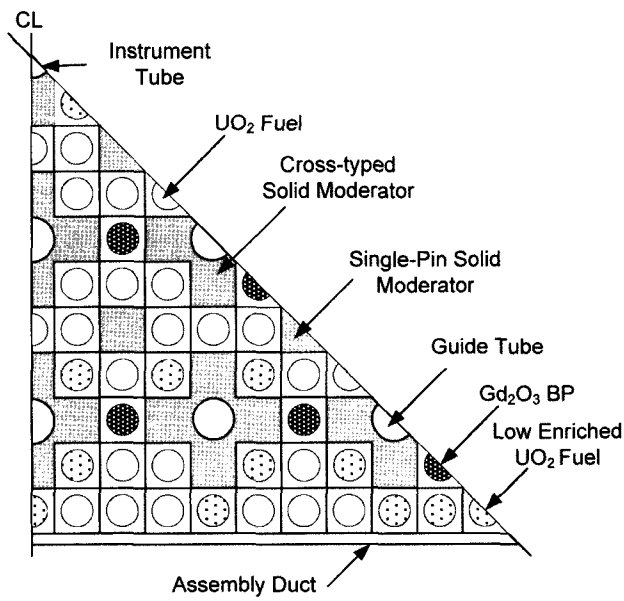

Fig. 6. Fuel Assembly Design.

pitch is 25.15 cm, including a 1 cm gap between the fuel assemblies. The fuel assembly is composed of 300 fuel rods, 25 cruciform-type solid moderator pins, and 16 single solid moderator pins. The pellet diameter and the outer diameter of the cladding are 0.82 cm and 0.95 cm, respectively. The clad material is a nickel-based alloy, which is highly resistant to stress corrosion cracking (SCC) at a supercritical water condition.

Since a high coolant density variation along the axial direction in an SCWR core induces a distortion of the axial power shape towards the core bottom, an axial zoning of the fuel enrichments, 6.5, 7.2, and 8.0 w/o from the bottom to the top of the core, is introduced to flatten the axial power shape. The heights of the three axial regions from the bottom to the top of the core are 85.2, 105.3, and 190.5 cm, respectively. In order to reduce radial pin peaking in the fuel assembly, a lower enriched fuel rod is also used near the corner of the fuel assembly or near the ZrH_2 solid moderators. In addition, the allocation of different number of burnable poison rods for the three axially divided zones would help to lower the axial power peaking. Fresh fuel assembly contains 32 gadolinia burnable poison rods in the bottom and the middle region of the core and 28 gadolinia rods in the top region of the core. The content of Gd_2O_3 in a gadolinia rod is 10 w/o.

3.3 Conceptual Core Design

3.3.1 Core Design Parameters

A feasibility study on the conceptual core design of an SCWR system has been performed at KAERI during the last 3 years. Basically, the design requirements of the conceptual SCWR core design were chosen based on the Gen-IV technical road map [1]. The power level of the conceptual SCWR core designed by KAERI is 1400 MW electric power generation. The conceptual SCWR core contains 193 fuel assemblies with a typical four-batch fuel-loading pattern. The design limit for the maximum linear heat generation rate is assumed to be 390 W/cm, which is the same as that of a light water reactor, while the average linear heat generation rate of the conceptual SCWR core is 144.2 W/cm. Therefore, the power peaking factor limit associated with the maximum linear heat generation rate is determined to be 2.7. A typical fuel-loading pattern for the equilibrium core with a four-batch reload scheme is shown in Fig. 7.

3.3.2 Orifice Design for a Flow Distribution

The maximum cladding temperature is limited to be less than 620°C to prevent corrosion and SCC under super critical water conditions for a fast system. In Japan, the maximum cladding temperature limit of 650°C was recommended by Yamaji et al. for a super critical thermal system for Nickel alloy [13]. At present, however, materials have not been selected for either the cladding or the structure and accordingly the temperature

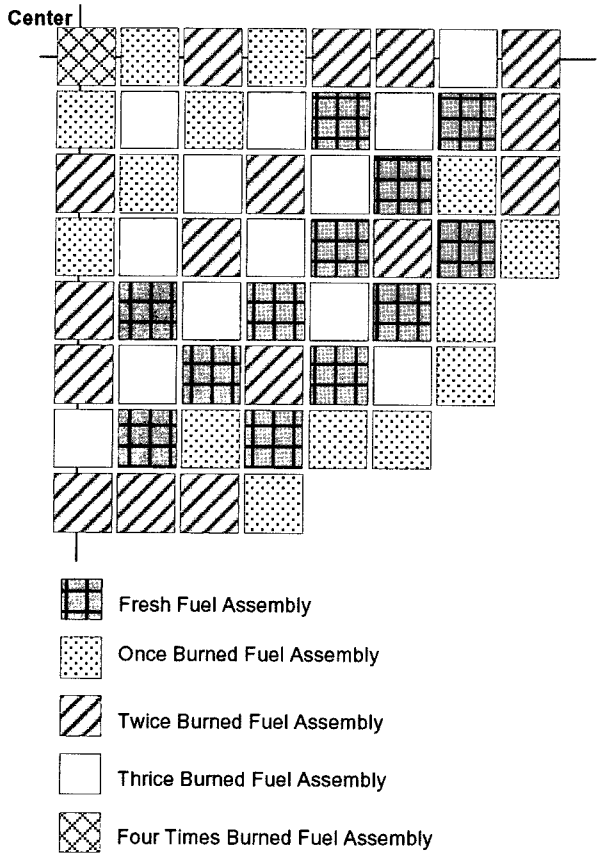

Fig.7. Four-Batch Core Loading Pattern

criteria have not been determined. In this study, the outlet coolant temperature of each assembly at the top of the core was calculated instead of the cladding surface temperature. The cladding surface temperature of the conceptual SCWR core will be analyzed by a sub-channel analysis as a future work. In order to reduce the coolant outlet temperature, an orifice concept to allow for a different flow rate for each assembly is introduced. The coolant flow rate distribution is determined by considering the assembly power distribution and the radial coolant temperature distribution. The optimized flow rates are presented in Fig. 8.

3.3.3 Control Banks Design

The SCWR core is operated with a boron-free condition, since it adopts a direct cycle without steam generators, steam separators, and steam dryers. Therefore, a control rod is solely responsible for excess reactivity control during a reactor operation period without soluble boron. Generally, the control rod driving mechanism (CRDM) is located at the top of the core in an SCWR system, similar to a conventional PWR, and is inserted from the top of the core during a core operating period, which can cause the axial power shape to become distorted and shifted to the bottom of the core on top of the possible power shape distortion due to a steep density decrease from the bottom to the top of a core. Control rod (CR) banks positions in the conceptual SCWR core are searched to minimize the power peaking factor, as shown in Fig. 9. Eight types of control banks were introduced, excluding a shutdown bank to control excessive

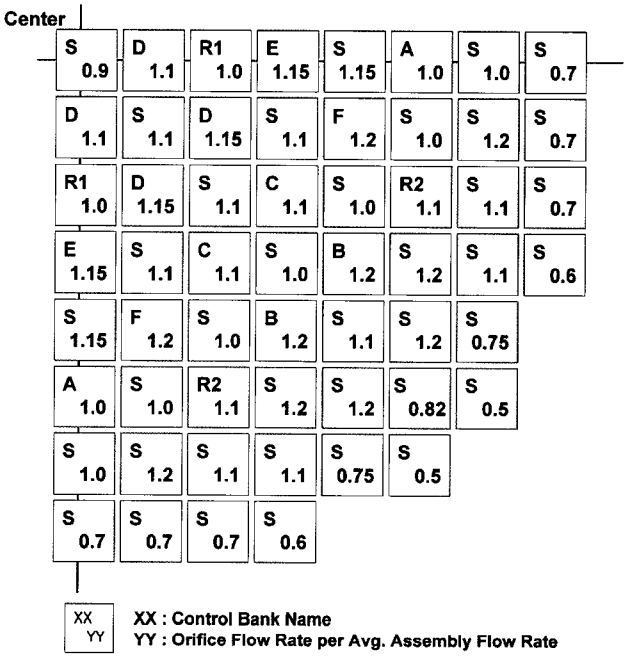

Fig. 8. Control Bank and Coolant Flow Rate of an Assembly

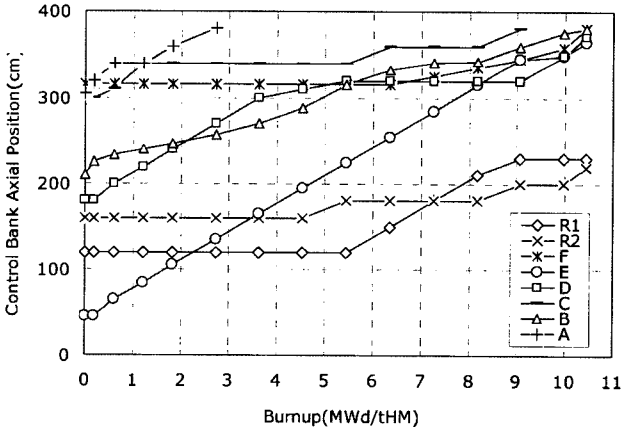

Fig. 9. Critical Control Bank Positions

reactivity and the power distribution. A neutron absorber material of 100 cm long, R bank, is introduced only for the axial power shape control, and the lengths of the absorber material region in the other control banks are the same as the fuel height. All the control banks are assumed to move individually without any systematic overlap mechanism. The critical position of the CR banks varies with the burnup and is depicted in Fig. 9.

3.4 Core Calculation Results

The core characteristics in this section are obtained from the core calculation for an equilibrium cycle. The average discharged fuel burnup of the SCWR core is 42 GWd/tHM. By using an enrichment zoning of the fuel in the three axial regions in a fresh fuel assembly, the axial power peaking factor can be managed to be less than 1.45 for a whole burnup period. In addition, the maximum power peaking factor is 2.45 at the BOC, which is much lower than the design limit of 2.7. The maximum coolant temperature was calculated as 577℃ at the BOC during a normal operation. Although the maximum coolant temperature is much lower than the design limit of 650℃, the exact cladding surface temperature should be analyzed via sub-channel analysis. The coolant temperature coefficient and fuel temperature coefficient are considered here to evaluate the inherent safety features of the conceptual SCWR core. Since a boron free operation is applied to the conceptual SCWR core, the coolant temperature coefficient is not heavily dependent on the core burnup. The coolant temperature coefficient varied from -22 pcm/℃ at the BOC to -23 pcm/℃ at the EOC. The coolant temperature coefficient here includes the effect of a coolant density change, and it implies that the coolant void coefficient of the conceptual SCWR core could become a negative value. The fuel temperature coefficient decreases slightly, from -2.0 pcm/°C at the BOC to -2.1 pcm/°C at the EOC, with an increase of the fuel burnup. As shown in Fig. 9, control banks to shutdown the reactor core are placed in the whole assembly, except for the positions of the control banks for power control. If a core-shutdown request failure occurs, both the shutdown control banks and the regulating control banks are inserted into the core. The shutdown margin for the conceptual SCWR core has been evaluated. The total control rod worth requirements, from hot full power (HFP) to cold zero power (CZP), includes the power defect from HFP to HZP, the xenon reactivity, and the excessive reactivity at HFP. The full core geometry model was used for the shutdown margin calculation in order to consider the stuck rod condition, where the most reactive control cluster was assumed to fail to be inserted into the core. The calculated shutdown margin of the conceptual SCWR core is 1.16, 2.39, and 3.54% $\Delta\rho$ at the BOC, MOC, and EOC respectively, which exceeds the shutdown margin requirement by 1% $\Delta\rho$ with a 10% uncertainty for the whole burnup period.

4. HEAT TRANSFER AT A SUPRCRITICAL PRESSURE

A heat transfer test loop, named as SPHINX (**S**upercritical **P**ressure **H**eat Transfer **I**nvestigation for **Ne**X**t** generation), has been constructed at KAERI [14]. The test loop uses carbon dioxide as a surrogate fluid for water. As a first step, a heat transfer test in single tubes and an annulus passage have been studied.

4.1 Experiment

The test facility was designed so that the heat transfer characteristics of supercritical CO_2 can be studied for various combinations of heat and mass fluxes at a given pressure. The pressure and temperature of CO_2 at critical point are 7.38 MPa and 30.98°C, respectively. For the details of the facility, readers are referred to a previous publication [14]. Fig. 10 shows the test sections and the locations of the measuring points. The test section at the left is a circular tube with an inside diameter of 4.4 mm and is heated by a direct current power supply to impose a uniform heat flux on the tube surface. To measure the wall temperatures , 41 K-type thermocouples, each 5 cm apart, are soldered on to the external surface of the tube. The section shown in the middle in Fig. 10 is a 9 mm tube test section. The details are the same as those for the 4.4 mm tube, except for the heated length. The section shown at the right is the test section for an annular passage. A heater rod of 8 mm OD is centered in the 10 mm ID tube. Twelve thermocouples are TIG welded spirally on to the surface of the heater rod with an axial distance of 100 or 200 mm and separated circumferentially at 60 degrees. The hydraulic diameter[2] of the annulus passage is 4.5 mm, which is almost the same as the 4.4 mm tube. The supercritical CO_2 flows upward, and the fluid temperatures are measured in the mixing chambers at the inlet and outlet of the test section. The tests were conducted with a change of the mass flux and heat flux at a given pressure. In order to investigate the effects of the pressure on a heat transfer, the experiments were performed at three different pressures: 1.05, 1.1, and 1.2 times the critical pressure. The outlet temperature of the test section is restricted to below 100°C for safety reasons. For each test, the heat flux at a given mass flux and the pressure are selected so that the fluid crosses the pseudocritical point inside the test section for an investigation of the heat transfer deteriorations. Table 1 shows the range of the test conditions.

[2] The concept of heated perimeter is introduced for the design of single heater with an annulus passage. With this concept the hydraulic diameter is calculated by $d_h=4A/P_{heated}$.

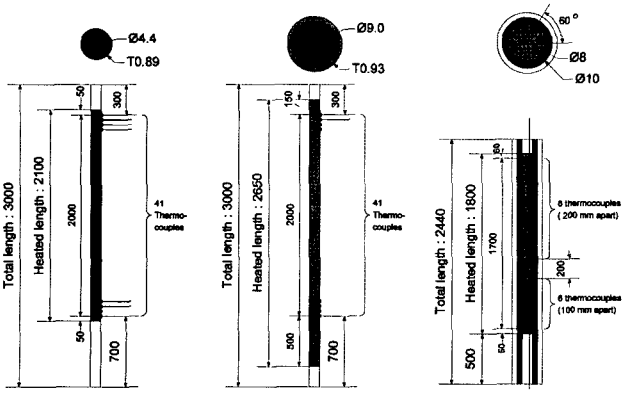

Fig. 10. Test Sections

Table 1. Test Conditions for the Heat Transfer at a Supercritical Pressure

Condition	Unit	Value
Inlet pressure	MPa	7.75, 8.12, 8.85 (1.05, 1.10, 1.15 P_{cr})
Inlet temperature	°C	5 ~ 27
Mass flux	kg/m^{2}s	400, 500, 750, 1000, 1200
Heat flux	kW/m^2	Up to 150

4.2 Heat Transfer Coefficient

Fig. 11 and Fig. 12 show the heat transfer coefficient (HTCs) for the 4.4 mm tube and the 9 mm tube. It is evident that, with the same test conditions, the HTC for a larger tube is lower than that for a smaller one. For 400 kg/m^{2}s and 30 kW/m^2, the occurrence of heat transfer deterioration is clearly shown for the 9 mm tube, while there is no deterioration for the 4.4 mm tube. The deterioration occurs early for the larger tube at a given combination of mass flux and heat flux.

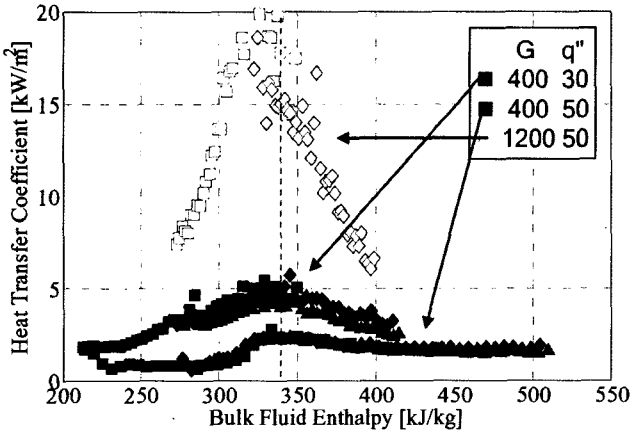

Fig. 11. Variation of the Heat Transfer Coefficients in a 4.4 mm Tube with Bulk Fluid Temperature for Several Combinations of Mass and Heat Flux

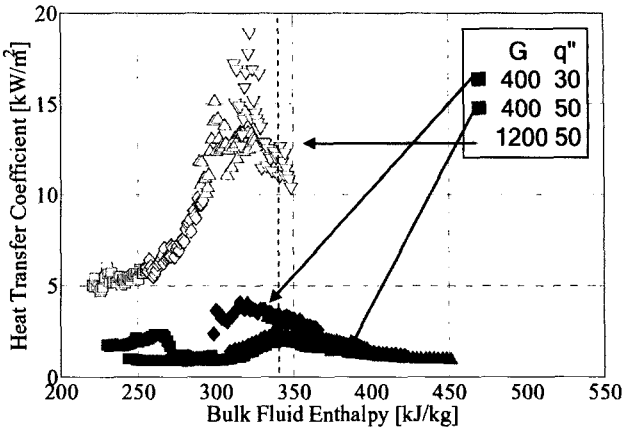

Fig. 12. Variation of the Heat Transfer Coefficients in a 9 mm Tube with Bulk Fluid Temperature for Several Combinations of Mass and Heat Flux

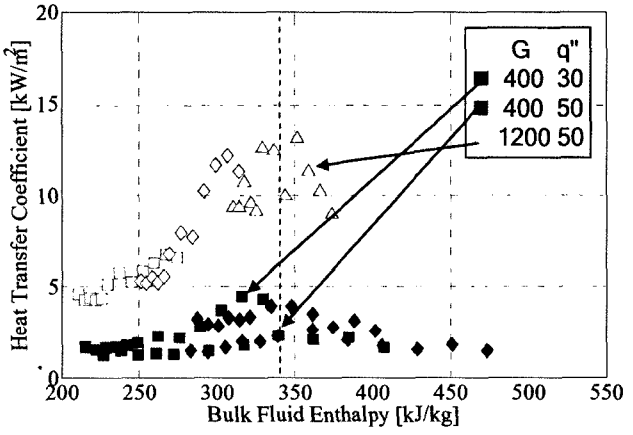

Fig. 13. Variation of the Heat Transfer Coefficients in an Annulus Passage of Equivalent Hydraulic Diameter of 4.4 mm with Bulk Fluid Temperature for Several Combinations of Mass and Heat Flux.

In Fig. 13, the HTCs for the annular passage (8 mm x 10 mm) are shown. Comparing the results of the annular passage with that of the 4.4 mm tube, it was found that the HTCs looked similar in the case of G=400 kg/m^2 s, but different in the case of G=1200 kg/m^2 s. We originally expected to obtain a very similar result for both of the geometries, since their hydraulic diameters were matched. However, the result was somewhat different. This disparity was probably due to the introduction of a

heated perimeter concept instead of a wetted perimeter, since the heated perimeter concept results in a narrower passage than the wetted perimeter concept does. The mechanism, however, is not fully understood and further research is required.

The experimental data for the tubes and single rod were analyzed to obtain the Nusselt number by considering both a forced and a mixed convection, where the effect of buoyancy is incorporated as a function of a buoyancy parameter. The Nusselt number takes the form shown in Eqs. (1) - (4).

$$Nu_b = Nu_{var} \cdot f\left(\frac{Gr_m}{Re_b^{2.7} Pr_m^{0.5}}\right) \tag{1}$$

where

$$Nu_{var} = 0.0183 Re_b^{0.82} Pr_b^{0.5} \left(\rho_w / \rho_b\right)^{0.3} \left(\overline{c_p} / c_{pb}\right)^n \tag{2}$$

The exponent is defined as follows.

$$n = \begin{cases} 0.4 \ for \ \dfrac{T_b}{T_{pc}} < \dfrac{T_w}{T_{pc}} \le 1 \ or \ 1.2 \le \dfrac{T_b}{T_{pc}} < \dfrac{T_w}{T_{pc}} \\ 0.4 + 0.2\left(\dfrac{T_w}{T_{pc}} - 1\right) \ for \ \dfrac{T_b}{T_{pc}} \le 1 < \dfrac{T_w}{T_{pc}} \\ 0.4 + 0.2\left(\dfrac{T_w}{T_{pc}} - 1\right)\left[1 - 5\left(\dfrac{T_b}{T_{pc}} - 1\right)\right] \ for \ 1 < \dfrac{T_b}{T_{pc}} < 1.2 \ and \ \dfrac{T_b}{T_{pc}} < \dfrac{T_w}{T_{pc}} \end{cases} \tag{3}$$

The function of the buoyancy parameter is defined for a normal heat transfer:

$$f\left(\frac{Gr_m}{Re_b^{2.7} Pr_m^{0.5}}\right) = \begin{cases} \left(1 + 476000 \dfrac{Gr_m}{Re_b^{2.7} Pr_m^{0.5}}\right)^{0.5} & if \ \dfrac{Gr_m}{Re_b^{2.7} Pr_m^{0.5}} < 8.5 \times 10^{-7} \\ 0.0476\left(\dfrac{Gr_m}{Re_b^{2.7} Pr_m^{0.5}}\right)^{-0.23} & if \ \dfrac{Gr_m}{Re_b^{2.7} Pr_m^{0.5}} < 3.3 \times 10^{-6} \\ 8.42\left(\dfrac{Gr_m}{Re_b^{2.7} Pr_m^{0.5}}\right)^{0.18} & if \ \dfrac{Gr_m}{Re_b^{2.7} Pr_m^{0.5}} < 7 \times 10^{-6} \\ \left(1 - 3000 \dfrac{Gr_m}{Re_b^{2.7} Pr_m^{0.5}}\right)^{0.295} & if \ \dfrac{Gr_m}{Re_b^{2.7} Pr_m^{0.5}} \ge 7 \times 10^{-6} \end{cases} \tag{4a}$$

and for a deteriorated heat transfer:

$$f\left(\frac{Gr_m}{Re_b^{2.7} Pr_m^{0.5}}\right) = \begin{cases} 1.16\left(1 + 550000 \dfrac{Gr_m}{Re_b^{2.7} Pr_m^{0.5}}\right)^{-0.36} & if \ \dfrac{Gr_m}{Re_b^{2.7} Pr_m^{0.5}} < 3.3 \times 10^{-5} \\ \left(3090 \dfrac{Gr_m}{Re_b^{2.7} Pr_m^{0.5}}\right)^{0.4} & if \ \dfrac{Gr_m}{Re_b^{2.7} Pr_m^{0.5}} \ge 3.3 \times 10^{-5} \end{cases} \tag{4b}$$

Fig. 14 shows the measured and predicted Nusselt number for the normal heat transfer mode (left) and the normal and deteriorated heat transfer modes (right). The dashed line indicates a $\pm 30\%$ error bound. It is noted that a considerable discrepancy occurs in the case of a deteriorated heat transfer mode. The initiating points of deterioration for various geometries are different from each other, and it was not possible to reduce all data with one correlation. The data beyond the $\pm 30\%$ error bound reflects this difficulty.

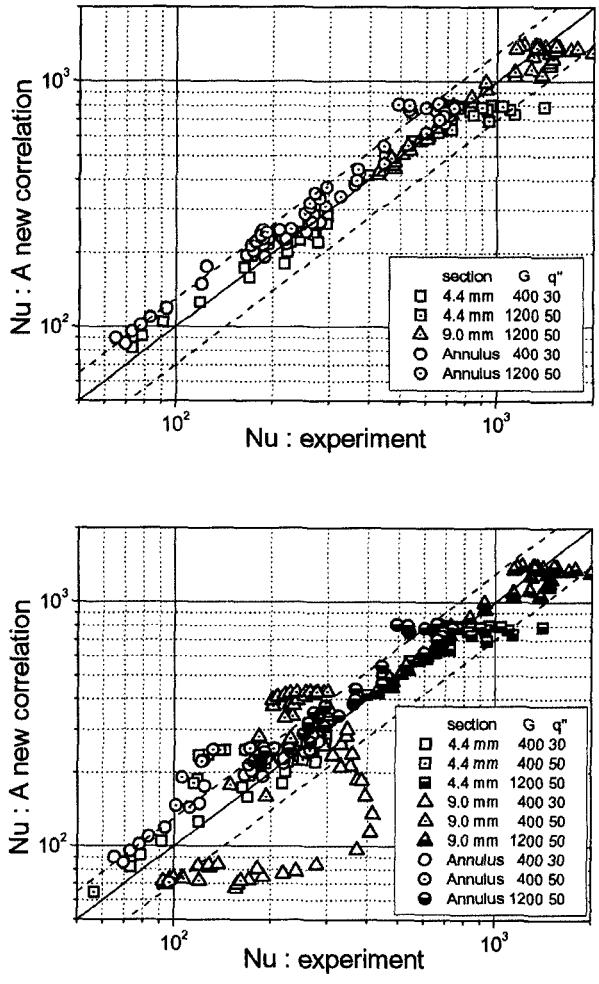

Fig. 14. Measured and Predicted Nu in the Case of a Normal Heat Transfer Mode (Left) and a Mormal and Deteriorated Heat Transfer Modes (Right)

5. SAFETY ANALYSIS CODE

A computer code, TASS/SCWR is under development for the safety analysis of an SCWR. It is based on TASS/SMR [15], which is a safety analysis code for the SMART, an integrated modular reactor. Relevant mathematical models are implemented for an application to supercritical water. Several test calculations have been carried out for a validation of TASS/SCWR.

5.1 Mathematical Models

For the modeling of a reactor coolant system, five one-dimensional conservation equations of a two-phase flow are formulated [16], where the thermodynamic properties are calculated by using the IAPWS-IF97 [17] formulation. The fission power input to the fuel is found from the reactor kinetics equations with six delayed neutron groups. An ANS73 decay heat curve has been incorporated into the database. Heat transfer correlations and conduction equations are modeled for a calculation of the heat generation in the core and the heat removal in the passive residual heat removal system (PRHRS).

5.2 Validation

A set of test calculations is performed for a simple geometry, as shown in Fig. 15, to validate the numerical models implemented in the TASS/SCWR. A series of natural circulation was simulated for a case where the average fluid temperature passed the pseudo-critical point. The calculated specific heat agrees well with the exact value (Fig. 16). For the last case, a natural circulation was simulated by using the TASS/SCWR and MARS

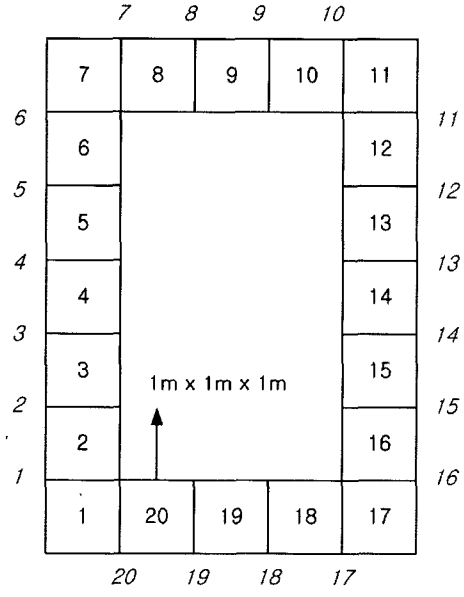

Fig. 15. Test Calculation Geometry

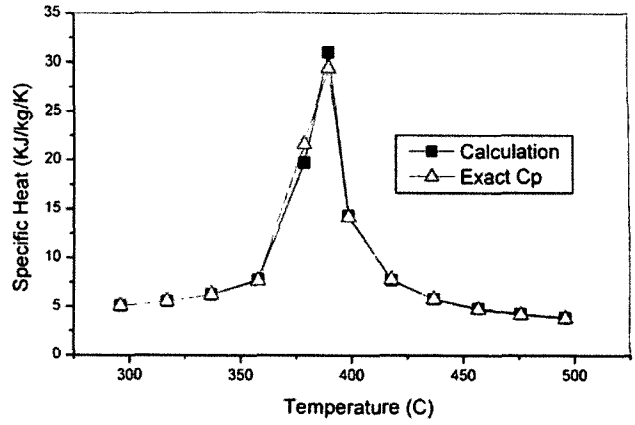

Fig. 16. Comparison of the Specific Heat

[18] codes, and the results were compared with each other. Initial pressure and temperature are 25 MPa and 300°C. Heat of 10 MW was supplied to node 2 and removed from node 12. The fluid density and temperature calculated by TASS/ SCWR and MARS, as shown in Fig. 17 and Fig. 18, were in good agreement with each other.

5.3. Passive Safety System for the SCWR

A passive safety system has been proposed for an SCWR. It is composed of a passive residual heat removal (PRHR) heat exchanger, a PRHR tank, and a compensation tank. A feasibility study on a passive safety system without a compensation tank has been performed [19], and the results showed that core cooling was important just after a feedwater loss. Fig. 19 shows the nodalization of TASS/SCWR for an SCWR with a PRHRS.

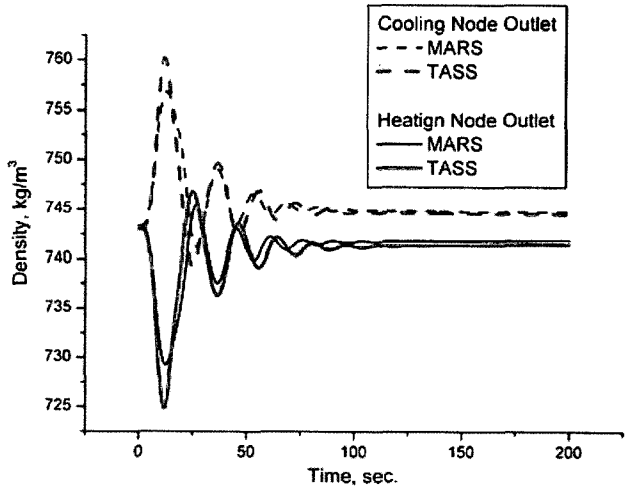

Fig. 17. Comparison of the Density

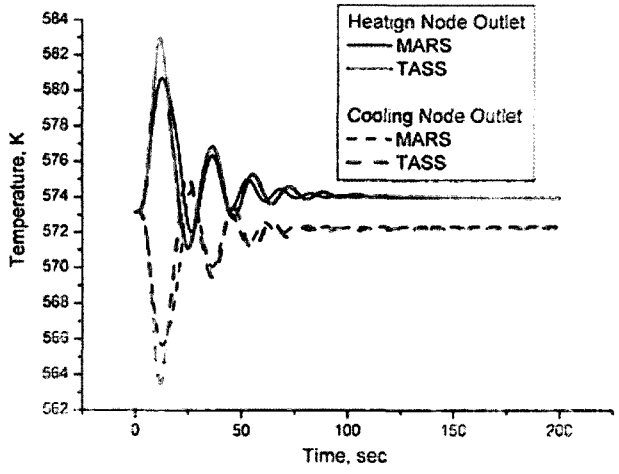

Fig. 18. Comparison of the Temperature

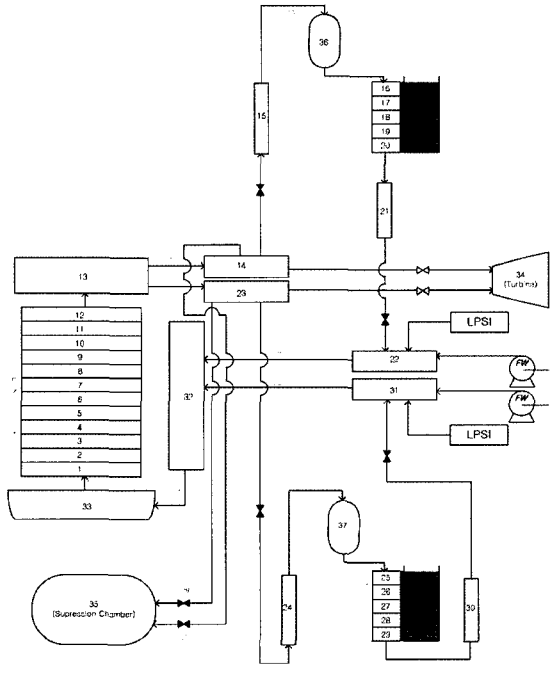

Fig. 19. Nodalization of the TASS for a SCWR

6. MATERIALS

For an application of the structural materials to the core internals or the fuel cladding, the candidate materials should be evaluated in terms of such properties as high temperature tensile strength, creep strength, corrosion and stress corrosion cracking susceptibility, radiation resistance, and weldability. Of such properties, in this work, corrosion tests for F/M steels and high Ni alloys have been performed in a supercritical water environment.

6.1. Experiment

Three groups of materials, F/M steels (T91, T92, T122), high Ni alloys (Alloy 625, 690, 800H), and an ODS alloy (MA 956, a commercial 20% Cr ODS alloy) were evaluated in a supercritical water environment. For a general corrosion rate measurement, specimen coupons of 10 x 10 x 2 mm were immersed in a supercritical water environment. The details of the specimens are summarized in Table 2. After the corrosion test, the weight change was measured, and the cross sections of the corrosion coupons were analyzed with a scanning electron microscope (SEM) and energy dispersive X-ray spectroscopy (EDS). The corrosion test loop for a supercritical water environment has been designed to operate up to 650°C and 30 MPa. It consists of a pressure vessel with a 3.3 liter volume capacity made of Hastelloy C-276, a make-up water control loop, a slow strain rate test (SSRT) driving and control unit, and a data acquisition module.

Table 2. Test Materials and the Conditions of the Coupons for the Corrosion Rate Measurements

Alloy Class	Alloy	Shape
Ferritic-Martensitic Steels	T91-I, T31-II T92, T122	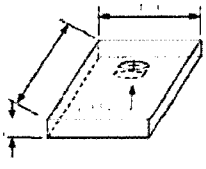
High Ni alloy (Superalloys)	Inconel625, Inconel690, Incoloy800H	
ODS alloy	MA956	

6.2 Corrosion Rate Measurement

The F/M steel specimens (T91, T92, and T122) showed a significantly higher corrosion rate than the high Ni alloys at 500°C, as shown in Fig. 20. The big difference in the corrosion rates between the two groups of alloys (F/M steels and high Ni alloys) seems to be due to the different dissolution behaviors of the main alloying elements, which is Fe for the F/M steels, and Ni for the

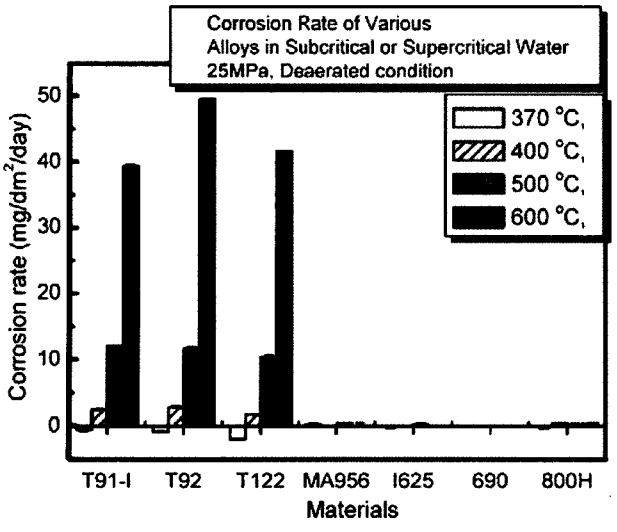

Fig. 20. Material Dependency of the Corrosion Rate of Various Alloys in Deaerated Subcritical or Supercritical Water

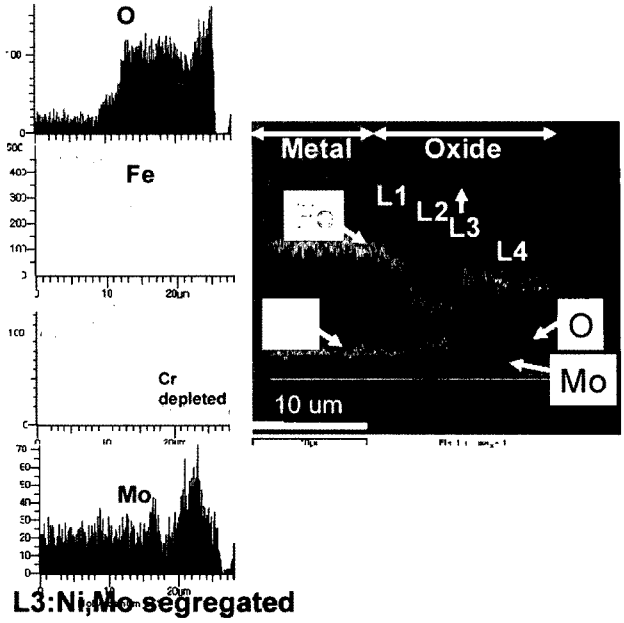

Fig. 21. Feature of the Oxide of the T91 Tested in a SCW at 550℃ in 25.5 MPa, DO < 10ppb

high Ni alloys. The corrosion rates of the F/M steels at 600°C appeared to be about three times higher than those at 500°C. At 370℃, a subcritical condition, the F/M steel specimens showed a weight loss instead of a weight gain at higher temperatures. Alloy MA 956 and the high Ni alloy specimens showed a small weight change before and after the immersion test in subcritical or supercritical water.

6.3. Corrosion Product Analysis

The oxide of the alloy T91 specimen was revealed to be composed mainly of three layers, as shown in Fig. 21. A thin layer (L3) was observed between layer 2 and layer 4, and it was found to be enriched with Mo and Ni. A distinct compositional variation was detected in layer 2 and layer 4: a depletion of Fe and an enrichment of Cr were shown in layer 2, and a depletion of Cr and an enrichment of Mo were detected in layer 4. Layer 3 enriched with Mo seems to retard the outward diffusion of the Cr atoms. The source of the Mo in layer 3 seems to be the alloying element of the T91 specimen and the test vessel material of Hastelloy C 276, a Ni-Cr-Mo alloy. An ion exchanger to purify the test solution was not installed for this corrosion test, so Mo atoms from the test vessel as well as from the T91 specimen could be dissolved and deposited onto the corrosion product. Alloy T92 and alloy T122 also showed a similar compositional profile with that of T91. On the surfaces of the MA 956, alloy 625, 690, and 800H specimens, thin oxides were observed. A very thin oxide was formed on the alloy 625 surface, and the main alloying elements did not seem to change near the surface. A previous report has also shown a similar test result for the corrosion of alloy 625 [20].

7. SUMMARY

This paper has described the research activities performed to date on an SCWR in Korea. These activities include a conceptual design of a coolant flow path, a conceptual design of a 1400 MWe SCWR core, the modification of a safety analysis code TASS/SCWR, an experimental study of a heat transfer at a supercritical pressure, and corrosion tests of candidate materials.

A SCWR-R concept has been proposed for a direct-cycle supercritical water-cooled reactor with an internal flow recirculation to reduce a hot channel maximum temperature while maintaining a higher coolant core outlet temperature. The concept is to achieve a high core flow rate and to reduce a burden on the BOP components simultaneously. The increased feedwater pressure supplies the driving momentum for the jet pump installed in the downcomer. A simplified one-dimensional thermal-hydraulic analysis showed that the cladding temperature of the hot channel for the SCWR-R is lower than the maximum allowable cladding temperature. A RETRAN jet pump model was utilized to size the throat area of the jet pump with the other parameters being fixed. The thermal efficiency calculated by considering the detailed heat balance of the steam cycle was 43.68 %.

The concept of an orifice manipulation for flow distribution control was found to be an effective approach to decrease the maximum coolant temperature to less than 586℃. The reactivity control by the control rods was confirmed to be applicable without violating the power peaking criteria.

The efforts to alleviate the high fuel cladding temperature have been approached from two different points of view, that is, thermal-hydraulics and core neutronics. Either approach assumed the parameters of the other as given and, thus, may have produced highly conservative outcomes. A future work should be an integrated conceptual design by considering every aspect of reactor core.

Heat transfer tests were performed for a vertically upward flowing CO_2 supercritical pressure in circular tubes and an annular passage. Heat transfer deterioration was observed at a low mass flux and a high heat flux. A new correlation was proposed.

The safety analysis code TASS/SCWR was modified for an application to an SCWR. A set of test calculations was carried out for the developed models. No serious mathematical or numerical problems were found during the test calculation, and the results of the TASS/SCWR and MARS codes showed a good agreement. TASS/SCWR is expected to be applied to the safety analysis of an SCWR with a PRHRS.

F/M steel specimens showed a higher corrosion rate in supercritical water than the high Ni alloys at 500 and 550℃. Corrosion rates of the F/M steels at 550℃ were about three times higher than those at 500℃. A thin layer composed mainly of Mo and Ni was observed between the two oxide layers, and it seems to retard the Cr diffusion into the outer layer of the corrosion product of the T92 and T122 specimens.

The data provided here is solely for research purposes and should not be construed as actual design data. The data used and generated during the course of the research described in this paper should be interpreted within the context of those individual research areas. There was never any attempt to check the consistency of, to integrate, or to summarize the design parameters.

ACKNOWLEDGEMENT

The authors would like to acknowledge the financial support of the Ministry of Science and Technology (MOST) of the Republic of Korea through the I-NERI program. The authors would also like to thank the Korea Atomic Energy Research Institute for providing an internal fund through its Fundamental Research Program.

REFERENCES

[1] A Technology Roadmap for Generation IV Nuclear Energy Systems, GIF-002-00, USDOE Nuclear Energy Advisory Committee and the Generation IV International Forum, December (2002).

[2] P. MacDonald, et al., "Feasibility Study of Supercritical Light Water Cooled Fast Reactors for Actinide Burning and Electric Power Production," INEEL/EXT-02-00925, Nuclear Energy Research Initiative Project 2001-001 (2002).

[3] X. Cheng, T. Schulenberg, "Heat Transfer at Supercritical Pressure - Literature Review and Application to a HPLWR," FZKA-6609, Forschungszentrum Karlsruhe GmbH, Karlsruhe (2001).

[4] Y. Oka, S. Koshizuka, "Concept and Design of a Supercritical -pressure, Direct Cycle Light Water Reactor," *Nucl. Tech.*, 103, 295 (1993).

[5] N. E. Petrov, V. N. Popov, "Heat Transfer and Hydraulic Resistance with Turbulent Flow in a Tube of Water at Supercritical Parameters of State," *Thermal Engineering*, 35, 10 (1988).

[6] *GESSAR II BWR Nuclear Island Design*, General Electric Company.

[7] *RETRAN-3D--A Programs for Transient Thermal-Hydraulic Analysis of Complex Flow Systems, Volume 1: Theory and Numerical Manual*, EPRI, Rev. 5 (2001).

[8] K. Dobashi, Y. Oka, S. Koshizuka, "Core and Plant Design of the Power Reactor Cooled and Moderated by Supercritical Light Water with Single Tube Water Rods,"*Ann. Nucl. Energy*, **24**, 16, 1281 (1997).

[9] R. Stammler et al., "User's Manual for HELIOS," Scandpower, (1994).

[10] B. O. Cho and C. H. Lee, "MASTER 2.0 User's Manual," KAERI/UM-3/98 (1998).

[11] H. K. Joo, J. W. Yoo and J. M. Noh, "A Conceptual Design for a Rectangular Fuel Assembly for the Thermal SCWR System," *Proc. GLOBAL2003*, New Orleans, LA, USA (2003).

[12] J. Buongiorno and P. E. MacDonald, "Study of Solid Moderators for the Thermal-Spectrum Supercritical Water-Cooled Reactor (Neutronics), *Proc. ICAPP2003*, Cordoba, Spain, May 4-7, 2003.

[13] A. Yamaji, Y. Oka, and S. Koshizuka, "Three-dimensional Core Design of High Temperature Supercritical-Pressure Light Water Reactor with Neutronic and Thermal-Hydraulic Coupling," *J. Nucl. Sci. Technol.*, **42**, 8, (2005).

[14] H. Kim, H. Y. Kim, J. H. Song, H. D. Kim, Y. Y. Bae, "Design and Progress of the SPHINX in KAERI", *Trans. KNS Spring Meeting*, Jeju, Korea, May 26-27, 2005.

[15] H. Y. Yoon et al., Thermal hydraulic model description of TASS/SMR, KAERI/TR-1835/2001, Korea Atomic Energy Research Institute, 2001.

[16] H. Y. Yoon, S. H. Kim, H. C. Kim, Y. Y. Bae, "Development of a Safety Analysis Code for a Supercritical Water Cooled Reactor (SCWR)," *Transactions of the Korean Nuclear Society Autumn Meeting* Busan, Korea, October 27-28, 2005.

[17] W. T. Parry, J. C. Bellows, J. S. Gallagher, A. H. Harvey, "ASME International Steam Tables for industrial use: Based on the IAPWS International Formulation 1997 for the thermodynamic Properties of Water and Steam (IAPWS-IF97)," CRTD- 58, ASME, 2000.

[18] B. D. Chung et al., MARS3.0 Code manual input requirements, KAERI/TR-2811/2004, Korea Atomic Energy Research Institute, 2004.

[19] H. Y. Yoon, Y. Y. Bae, Feasibility Study of a Passive Safety System for a Supercritical Pressure Water Cooled

Reactor, *Proceedings of GENES4/ANP2003*, Sep. 15-19, Kyoto, Japan, 2003.

[20] S. Teysseyre, et al., "Corrosion and stress corrosion cracking of austenitic alloys in supercritical water", *Proceedings of 11th International Symposium on Environmental Degradation of Materials in Nuclear Power Systems-Water Reactors*, Stevenson, WA, USA, Aug. 10-14, 2003.